Atom Indonesia

Journal homepage: http://atomindonesia.brin.go.id

The Effect of Loop Inclination on Natural Circulation Mass Flow Rate and Heat Removal Inside Rectangular Passive Cooling Loop

N. R. Budiyanto[1], Deendarlianto[1], D. Yuliaji[1,3], R. Oktaviandi[1], E. P. A. Raharjo[1], S. A. Maryadi[1], A. E. Pamungkas[2], P. H. Setiawan[2], A. A. Budiman[2], M. Juarsa[2*]

[1]*Department of Mechanical and Industrial Engineering Faculty of Engineering, Gadjah Mada University, Jl. Grafika No. 2, Yogyakarta 55281, Indonesia*
[2]*Nucler Reactor Thermal-Fluids System Research Group, Research Center for Nuclear Reactor Technology, Research Organization of Nuclear Energy, Gd.80 KST B.J. Habibie, Setu Tangerang Selatan 15314, Indonesia*
[3]*Department of Mechanical Engineering, Faculty of Engineering and Science, Ibn Khaldun Bogor University, Jl. Sholeh Iskandar Kedungbadak, Kota Bogor 16162, Indonesia*

ARTICLE INFO

Article history:
Received 21 May 2024
Received in revised form 10 April 2025
Accepted 14 June 2025

Keywords:

Inclination angle
Natural circulation
Passive cooling
Heat removal
Mass flow rate
FASSIP-04 Ver.0

ABSTRACT

The use of passive cooling systems as a reactor safety measure has become a key approach to preventing future incidents similar to the Fukushima Daiichi NPP accident. These systems operate based on natural circulation, a process driven by temperature differences and elevation between the heat source and heat sink. Key design factors, such as the inclination angle of the rectangular loop, significantly influence this circulation. This study aims to investigate the effects of different inclination angles of the rectangular loop and variations in the initial water temperature in the Water Heating Tank (WHT) on the flow rate and heat removal capability. The research was conducted experimentally using a natural circulation rectangular loop facility, FASSIP-04 Ver.0, which has an inner diameter of 26.64 mm, a rectangular loop height of 2280 mm, and a width of 780 mm. The experimental variations were achieved by adjusting the water temperature inside the WHT to 50°C, 70°C, and 90°C. Meanwhile, the inclination angle of the loop was set to 30°, 60°, and 90° mass flow rate and heat removal capability was influenced by both the loop inclination angle and the water temperature in the WHT. The highest values were observed at a 90° inclination angle and a set temperature of 90°C, with a mass flow rate of 0.0241 kg/s, and heat removal rates of qH = 0.791 kW, qC = 0.489 kW. The resulting buoyancy force was stronger under these conditions, leading to greater heat removal through natural circulation compared to free convection, thereby increasing both mass flow rate and heat removal efficiency.

INTRODUCTION

The Nuclear Power Plant (NPP) accident that occurred on March 11, 2011, at the Fukushima Daiichi NPP in Japan was caused by a 9.1-magnitude earthquake. The damage to the electrical supply equipment occurred because it was submerged by the tsunami. The flooding affected units 1 to 6 of the NPP, and the damage to the power system resulted in a Station Blackout (SBO). As a result, the Active Cooling System (ACS) failed to cool the reactor core, causing the fuel to melt due to the temperature increase resulting from fuel decay [1,2]. Based on this accident, researchers developed passive safety systems for nuclear power plant thermal management, with one of their components being the Passive Cooling System (PCS) [3]. The PCS is utilised in several engineering applications such as solar water heaters, geothermal, and nuclear safety systems [4]. The one application of a passive safety system is to cooling-down reactor core over-heated such as a Light Water Reactors (LWRs) during transient cooling after the accident conditions [5]. A deeper understanding of natural circulation flow in cooling systems is essential

*Corresponding author.
E-mail address: mulya.juarsa@brin.go.id
DOI: https://doi.org/10.55981/aij.2025.1467

for enhancing the safety of nuclear power plants, both during normal operation and in accident scenarios. Studying this phenomenon helps optimise the efficiency of passive cooling systems, ensuring better thermal regulation and improved accident mitigation [6].

The Passive Cooling System (PCS) operates based on natural laws, relying on the Natural Circulation (NC) phenomenon that occurs in the absence of external forces [7-9]. Various thermal-hydraulic parameters influence the efficiency of natural circulation. In a reactor, natural circulation for core heat removal occurs due to the density variation between the descending cold fluid in the downcomer and the heated or two-phase flow rising within the core, a phenomenon driven by buoyancy forces. Various thermal-hydraulic factors determine the effectiveness of natural circulation. It is driven by density differences and buoyancy forces between descending cold fluid in the downcomer and rising heated or two-phase flow within the core [10]. The natural circulation phenomenon occurs due to buoyancy forces, which are influenced by density differences and gravitational forces acting over the height difference between the heating section and the heat sink [11]. Thus, PCS research has been conducted using various methods based on pressure differences, temperature variations, and geometric modifications [12,13]. In passive systems, the heat removal process is primarily influenced by fluid flow characteristics, which dictate the efficiency of natural cooling [14]. Among these characteristics, the effectiveness of natural circulation depends on the mass flow rate. Various factors, including geometry, working fluid properties, power input, and loop height, influence the magnitude of the mass flow rate. Among the geometrical parameters, height plays a crucial role in analysing the mass flow rate based on the loop's elevation. The difference in height can be divided by geometrical and inclination loops.

Several studies have investigated natural circulation flow rates with different loop heights. Cheng et al. (2023) conducted an experiment on [15] experimented on reducing flow distortion using loop facilities with different maximum heights of 16 meters, 8 meters, and 4 meters. The results showed that variations in power input and loop height affected the mass flow rate, with higher loop heights and power inputs leading to increased flow rates [15]. In addition to geometry, another factor influenced by height is the orientation of the heat source and heat sink. The position of the heat source significantly affects the magnitude of the natural circulation flow. A study conducted by Chen et al. (2014) indicates hat the orientation of the heat source in a vertical position results in a more stable heat flux than in a horizontal position, thereby influencing the buoyancy force on the hot side [16]. The flow rate performance is maximised in the Horizontal Heater-Horizontal Cooler (HHHC) configuration compared to the vertical Heater-Vertical Cooler (VHVC) configuration [17]. The largest natural circulation flow rate when varying the orientation of the heat source and heat sink positions in the rectangular loop occurs at the HHHC position [18]. The asymmetrical position of the heat source and heat sink, such as Horizontal Heater Vertical Cooler (HHVC) and Vertical Heater Horizontal Cooler (VHHC), causes differences in the flow direction [19].

Thermal performance in natural circulation is influenced by the vertical distance between the heat source and the heat sink. A study conducted by [20] with a HHHC configuration showed that a 75° inclination increased the heat source temperature and reversed the flow direction. A 15° tilt from the vertical axis on the loop can reduce flow instability in asymmetric loops [21]. Increasing the loop tilt results in an increase in the friction factor and a decrease in buoyancy [22]. Meanwhile, another research with variations in slopes of 0^o, 45^o, and 90^o, the effect of heat transfer values with pipes using SS316 material with a diameter of 1 inch was analysed, and experimental results increased the mass flow rate of water [23]. The inclination loop on thermal performance that occurred in observed stable behaviour for water, and thermal performance decreases with increasing inclination angle and increases with coolant temperature [24]. The research on counterclockwise inclination loop showed higher MFR than clockwise inclination due to a higher effective height difference between heater and cooler at the same inclination angle [25].

Based on the above description, this research focuses on the natural circulation phenomenon by analysing mass flow rates and heat removal as a function of loop inclination angle changes. We expect that the research data can contribute to the development of PCS capabilities. Innovations in thermal management within PCS are essential to help prevent similar accidents in the future.

METHODOLOGY

Analytical method

This research was carried out experimentally by analysing the calculation results obtained through a data acquisition system in the data output are NC flow rate (measured by EM

flowmeter) and temperature data (measured by thermocouples). The calculation of mass flow rate and heat removal calculations can be done by using NC flow rate and temperature changes data using Eq. (1).

$$\dot{m} = Q\rho \quad (1)$$

The volume of water flowing in a pipe channel or the product of the water discharge and the fluid density is the mass flow rate of water by calculating the average speed of water passing through a cross-sectional area using the Eq. (2).

$$Q = Av \quad (2)$$

The flow discharge value is then used to calculate the average speed of the flowing fluid using the Eq. (3).

$$v = \frac{Q}{A} \text{ (TH-in and TH-out) [26]} \quad (3)$$

Because, in this study, density is a function of temperature, the density value can be obtained using T_{avg} (TH-in and TH-out) [26] and the Eq. (4).

$$\rho = \left(A + BT_F + CT_F^{\,2}\right) \quad (4)$$

Where :

ρ : liquid density (kg/m^3)
T : temperature (^{o}C)
A : 1004.789042
B : -0.046283
C : -7.9738 x 10^{-4}
T_F : 1.8T_{avg} + 32

Changes in temperature affect the specific heat capacity (c_p) of water, which can be calculated using the Eq. (5) [26].

$$c_P = \left[\frac{(A+CT)}{(1+BT+DT)}\right] \quad (5)$$

Where :

c_p : liquid specific heat (kJ/kg.^{o}C)
T : temperature (^{o}C)
A : 17.48908904
B : -1.67507 x 10^{-3}
C : -0.03189591
D : -2.8748 x 10^{-6}

After knowing the value of the mass flow rate of water, the value of heat removal by water is determine based on Eqs. (6) and (7).

$$q_H = \dot{m}_H c_P\left(T_H\right)\Delta T_H \quad (6)$$

$$q_C = \dot{m}_C c_P\left(T_C\right)\Delta T_C \quad (7)$$

This research was expected to analyse the effect of the rectangular loop's inclination angle on the flow rate and the amount of heat removal.

Experimental method

Experimental facility FASSIP-04 Ver.0 is a research facility that utilised natural circulation phenomenon caused by the temperature differences of heater WHT and cooler WCT. Experimental setup is depicted in Fig. 1. If the heat is produced, the heat exchanger pipe in the cooling tank containing water at a cooling temperature is circulated by a pump so that the heat produced will be removed. The sensor installed on the research tool is a thermocouple and magnetic flowmeter. The instrumentation and control system during the experiment was carried out using the National Instrument Data Acquisition System (NI-DAS). The experimental setup records temperature and flow rate data of the WHT and WCT at different inclination angles. Temperature measurements are typically taken at six designated points (TH-OUT - TH-IN, TC-IN - TC-OUT) along the loop to determine the value of the difference in temperature characteristics and mass flow rate.

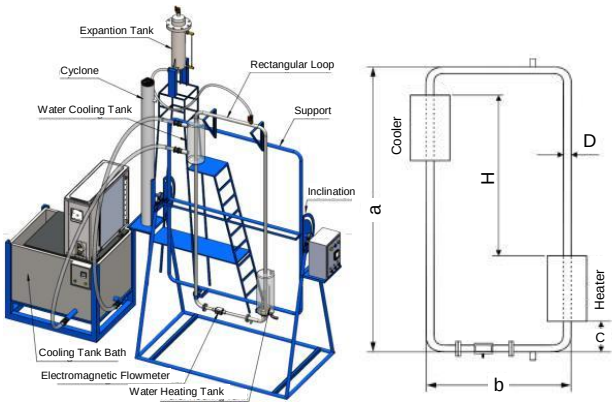

Fig. 1. Rectangular loop FASSIP-04 Ver.0.

The main geometry specification is provided in Table 1 and the schematic diagram of the setup shown in Fig. 2.

Table 1. Parameter geometry data.

Item	Symbol	Value/Material
Loop height	*a*	2280 mm
Loop width	*b*	780 mm
Position heater and cooler	*c*	160 mm
Effective length	*H*	1550 mm
Outside diameter	D_{out}	33.4 mm
Inside diameter	D_{in}	30.02 mm
Total length loop	*Lt*	6120 mm
The volume of fluid in the loop	mL	4300 millilitres
Heating power	kW	1.5 kW
Cooling power	2	kW
Temperature sensor	^{o}C	Thermocouple type K
Current Sensor	LPM	Electromagnetic Flowmeter

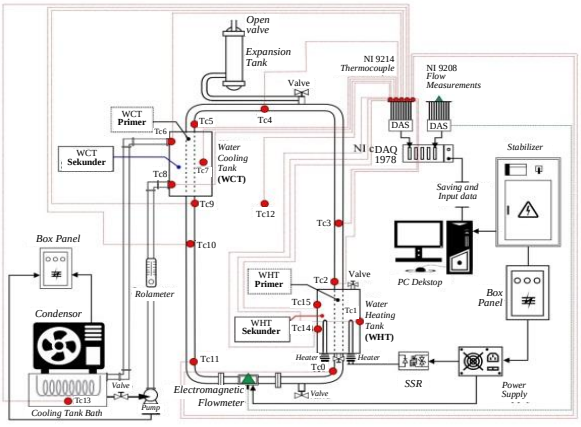

Fig. 2. Schematic diagram of experimental apparatus.

Table 2. Main thermocouple inputs in the analysis mass flow rate and heat removal.

Module	Channel	Description	Position
NI 9214	TC00	TH-IN	bottom of the heating tank
	TC01	T-HT	the middle section of a heating tank
	TC02	TH-OUT	top of the heating tank
	TC05	TC-IN	top of the cooling tank
	TC07	T-CT	cooling tank centre section
	TC09	TC-OUT	the bottom of the cooling tank
NI 9208	TC01	EH-Flow	flowmeter part

Table 2 provides an overview of the thermocouple placement within the experimental setup, detailing the assigned channels and their corresponding measurement locations. The placement of thermocouples has been determined at the temperature measurement points that indicate temperature changes in the hot part (WHT) and in the cold part (WCT) to determine the magnitude of the thermal energy changes that occur during experiment.

Figure 3 describes the research working flow:

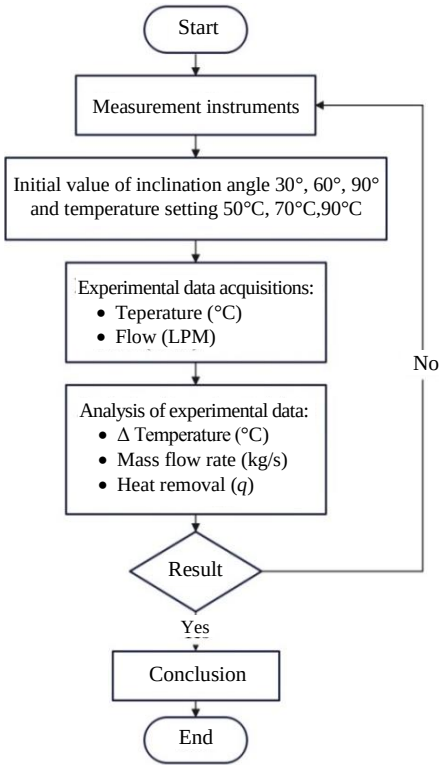

Fig. 3. Research flow diagram.

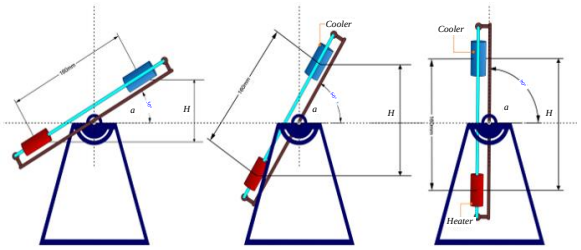

(a)

(b)

Fig. 4. Variation inclination rectangular loop 30^{o}, 60^{o}, and 90^{o} (a) schematic, (b) experimental.

Experimental variations were determined by changing the water temperature in the WHT to 50°C, 70°C, and 90°C. Meanwhile, the inclination rectangular loop (α) was varied from 30°, 60°, and 90^{o}. The cooler was turned on at a constant temperature of 10°C. Then, the heater temperature variation was set to 14000 s. Each angle of inclination loop is shown in Fig. 4.

RESULTS AND DISCUSSION

The experimental results, shown in Fig. 5 and Table 3, present the temperature and time characteristics required to reach steady-state conditions at various angles of inclination (30°, 60°, and 90°) of the rectangular passive cooling loop. For each variation ininclination angle, the system reached steady-state conditions and was maintained for up to 14,000 seconds, with the corresponding steady-state time (t) presented in seconds (s) for each configuration.

Table 3. Steady-state period time in various inclination angles and temperature conditions of WHT.

Inclination angle (α)	Temperature		Steady-state (*t*)
	WHT (°C)	WCT (°C)	
30°	50	10	780 s
	70	10	1814 s
	90	10	2598 s
60°	50	10	834 s
	70	10	1814 s
	90	10	2760 s
90°	50	10	1054 s
	70	10	2456 s
	90	10	2836 s

Temperature differences profile

The measured ΔTH in the WHT and WCT sections at different inclinations showed the fluid flow phenomena under varying temperature settings of 50°C, 70°C, and 90°C for TH variation (Fig. 5) and for comparison of the average temperature (Fig. 6).

Based on Fig. 5, an increase in the WHT temperature setting affected the temperature difference between its inlet and outlet. WHT temperature settings of 70°C and 90°C showed similar pattern, but a different pattern was observed at a WHT temperature setting of 50°C. A small inclination value, in this case, 30°, resulted in a smaller water temperature difference between the WCT and WHT compared to the 60° and 90° inclinations. This occured because the vertical groove in the hot arm section was shorter at an inclination of 30°, which reduced the buoyancy force and consequently increased heat losses along the pipe from the WHT to the WCT. From the observations, the highest average temperature difference was obtained at a inclination of 30°, while the lowest was at 60°. However, each temperature change exhibited different wavelengths and densities, with ΔTH increased in magnitude as the inclination varied. In addition, at an angle of inclination of 30°, temperature variations of 70°C and 90°C showed overshoot behavior when reaching steady-state conditions. Based on a comprehensive observation of Fig. 5, the average temperature difference between the inlet and outlet of the WHT can be summarized in Fig. 6.

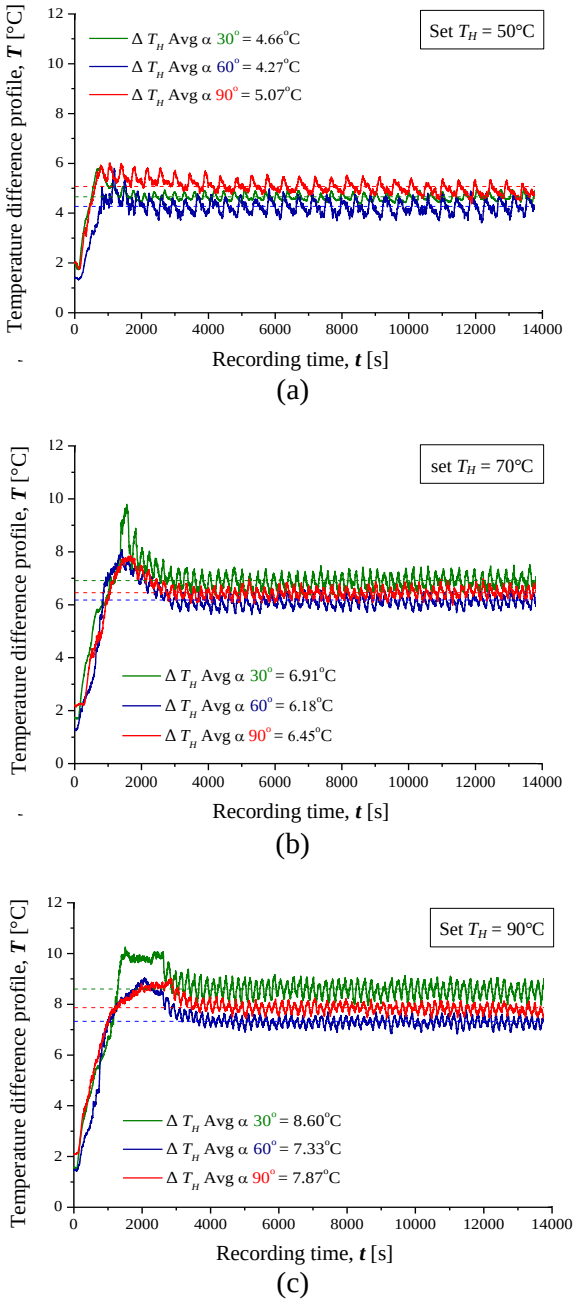

Fig. 5. Water temperature difference profile between the WHT variation inclination angles and set temperatures.

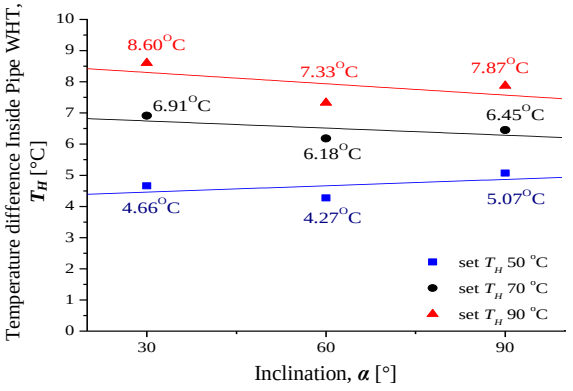

Fig. 6. Temperature difference inside pipe WHT based on variation inclination.

Changes in inclination during the experiment affected the ΔT WHT, as shown in Fig. 7. Increasing the inclination from 30° to 90° resulted in a decrease in ΔT WHT at temperature settings of 90°C and 70°C, although a slightly different pattern was observed at 60° inclination. A distinct pattern was also observed at the 50°C setting, where no decrease in ΔT WHT occurred, likely influenced by ambient temperature during the experiment. The decrease in ΔT WHT with increased inclination may attributable to reduced friction factors. Geometrically, the friction factor reaches its lowest value at a 90° inclination.

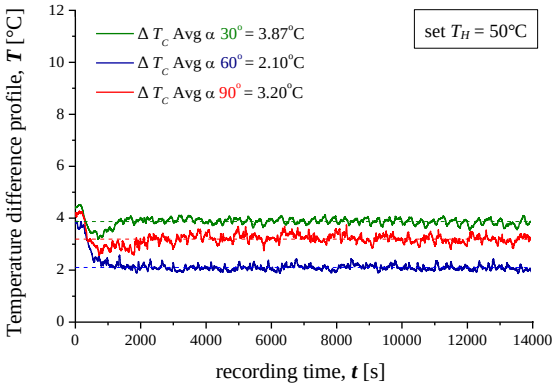

(a)

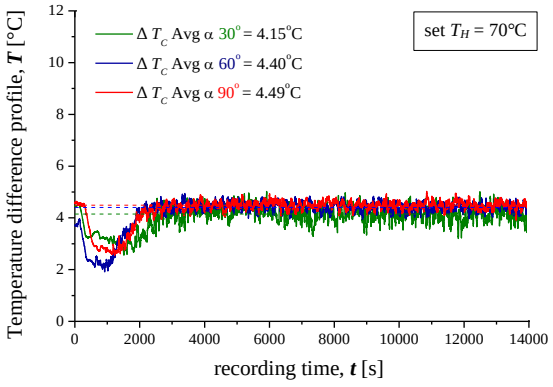

(b)

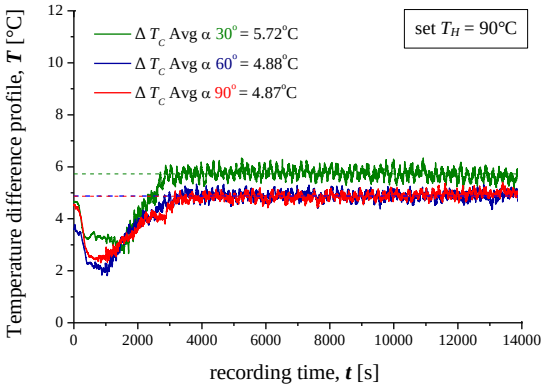

(c)

Fig. 7. Water temperature difference profile between the WCT variation inclination angles and set temperatures.

The temperature difference between WHT and WCT for all experiments is shown in Fig. 7. Temperature undershoot observed as shown in Figs. 7(a), 7(b), and 7(c) occured due to the transient heating process, until reaching the steady-state condition, for TH temperature setting variation from 50°C, 70°C, and 90°C, respectivelly. In the initial phase, the cooling system was set to maintain a temperature difference of 10°C with a cooling flow rate of 3 LPM, ensuring stable heat removal from the WHT to the WCT under steady-state conditions. During the phase leading up to steady-state, a temporary temperature drop (undershoot) occured. This phenomenon occurred due to a sudden increase in temperature in the WHT and hot pipes before the fluid eventually began to circulate and the temperature returned to the transient heating condition.

Meanwhile, each temperature adjustment provided by the cooler tank to the loop resulted in a corresponding change in ΔTC. At 50°C, the temperature difference varied significantly with each change in loop inclination, as shown in Fig. 8. In contrast, at 70°C, the variation in temperature difference was relatively small. At 90°C, the temperature difference became notably larger at inclinations of 60° and 90°.

As shown in Fig. 8, the decrease in temperature inside the WCT pipe was caused by an increase in the angle of inclination in each experiment. Increasing the inclination toward 90° enhanced the buoyancy force and mass flow rate, causing the temperature in the WCT to decrease further. This phenomenon was observed at WCT temperature settings of 50°C and 90°C. However, at the WHT temperature setting of 70°C, the behavior differed: the temperature difference values were 4.15°C, 4.40°C, and 4.49°C t inclination angles of 30°, 60°, and 90°, respectively.

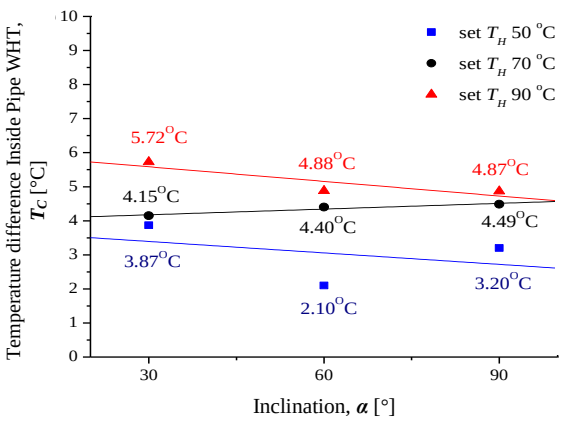

Fig. 8. Temperature difference inside pipe WCT based on variation inclination.

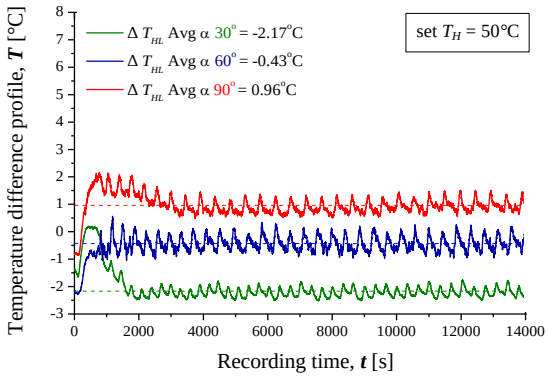

(a)

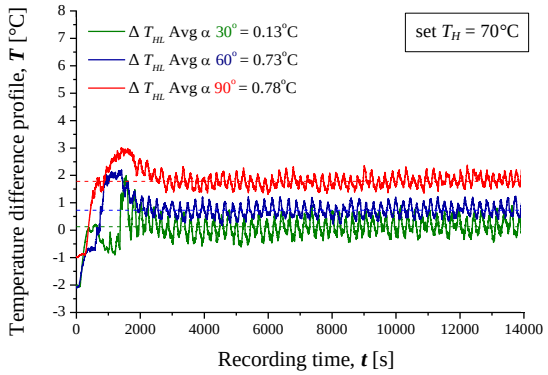

(b)

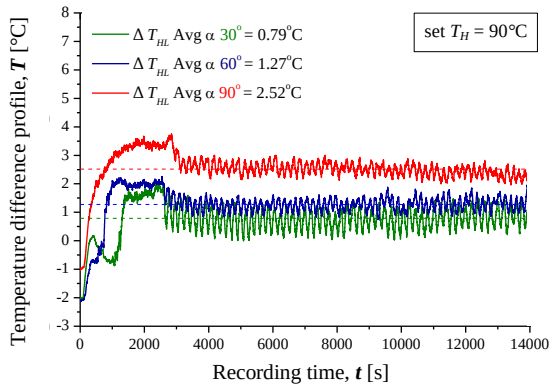

(c)

Fig. 9. Profile temperature ΔTHL inside hot-leg.

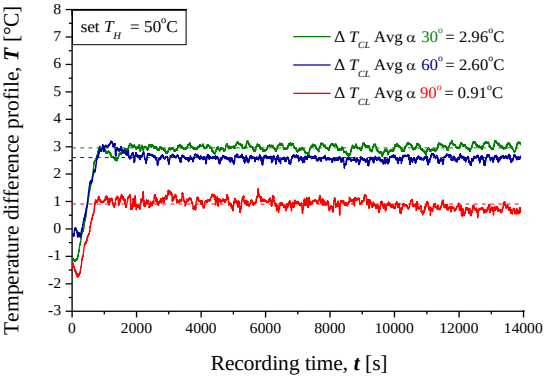

(a)

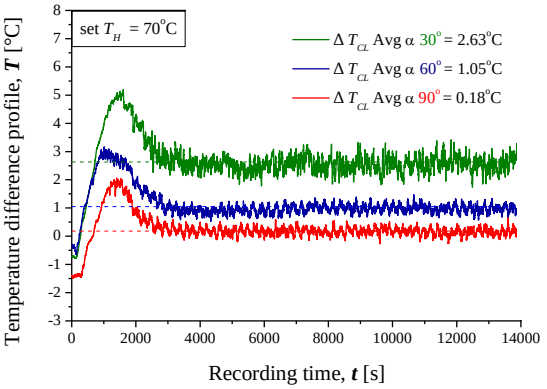

(b)

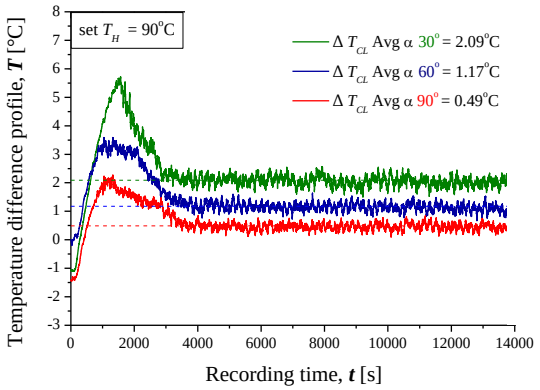

(c)

Fig. 11. Profile temperature ΔTCL inside cold-leg.

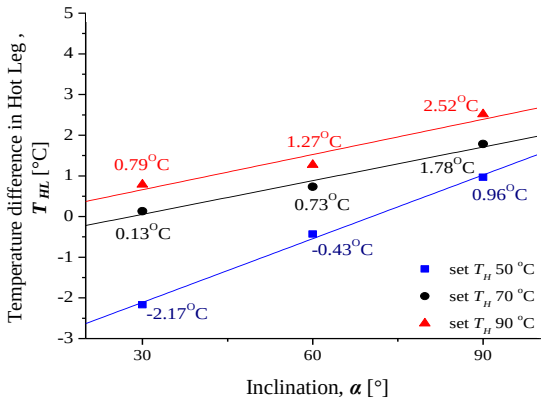

Fig. 10. Temperature difference in hot-leg.

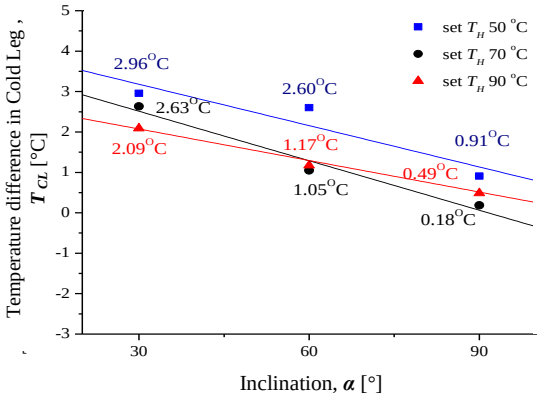

Fig. 12. Temperature difference in cold-leg.

Furthermore, changes in the temperature profile of the ΔTHL section can be seen in Fig. 9. It is known that temperature changes applied to the Hot-leg section of the loop result in variations in ΔTHL, as shown in Figs. 9(a), 9(b), and 9(c). However, the thermal response at a temperature of 50°C with inclination angles of 30° and 60° had a fairly large temperature difference for each change in the loop's inclination angle.

Figure 10 showed the temperature difference in the hot leg, which arose due to the temperature gradient. At a temperature setting of 50°C, the temperature difference was lower compared to the 70°C and 90°C settings. This lower difference was attributed to the relatively low buoyancy force at 50°C. At 70°C and 90°C, the temperature patterns were similar, with only minor differences observed between inclination angles of 30° and 60°.

Based on Fig. 11, the thermal response in the cold-leg section differed significantly. At the temperature setting of 50°C (Fig. 11a), the average temperature difference in the cold leg was nearly the same at tilt angles of 30° and 60°, while at 90° the average temperature difference was lower. This pattern was not repeated at the 70°C and 90°C settings (Figs. 11b and 11c). These differences indicate that the effect of tilt angle on the cold-leg temperature difference varied with the temperature setting.

The differences in the hot-leg temperature patterns are more clearly illustrated in Fig. 12. A linear intersection occurred at the temperature settings of 70°C and 90°C, whereas at 50°C the intersection was positioned above both lines. The linear intersection at 70°C and 90°C indicates that changes in the dynamic viscosity of water in the cold-leg section produced an inverse effect as the tilt angle increased. This phenomenon was attributed to increased heat absorption at the top, particularly at a 30° inclination, which reduced the influence of the mass flow rate.

Mass flow rate characteristics

The mass flow rate at temperature settings of 50°C, 70°C, and 90°C showed differences in the flow produced in the WHT, WCT, hot-leg, and cold-leg sections. Changes in the mass flow rate were influenced by the loop inclination angle, which altered the friction factor of the water inside the pipe and contributed to variations in NC flow. The mass flow rate variations at the input temperature settings of 50°C, 70°C, and 90°C are shown in Fig. 13.

As shown in Fig. 13a, the average mass flow rate of 0.0111 kg/s was the highest at a WHT temperature of 50°C for a loop inclination of 90°. At 30°, the mass flow rate differed notably from those at 60° and 90°, with a deviation of approximately ±0.0025 kg/s. At a WHT temperature of 70°C, the highest mass flow rate of 0.0175 kg/s occurred at 90°, while the lowest was observed at 30° (Fig. 13b). For a WHT temperature of 90°C, Fig. 13c shows that the maximum mass flow rate reached 0.0240 kg/s, while the minimum occurred at 30°, with a difference of ±0.00485 kg/s between the 60° and 90° inclinations. Based on Fig. 13, the comparison of mass flow rates for each inclination is summarized in Fig. 14.

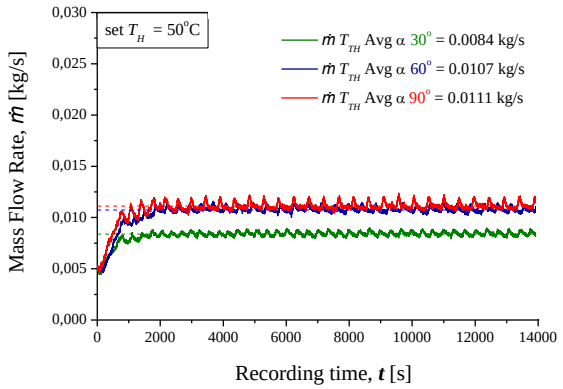

(a)

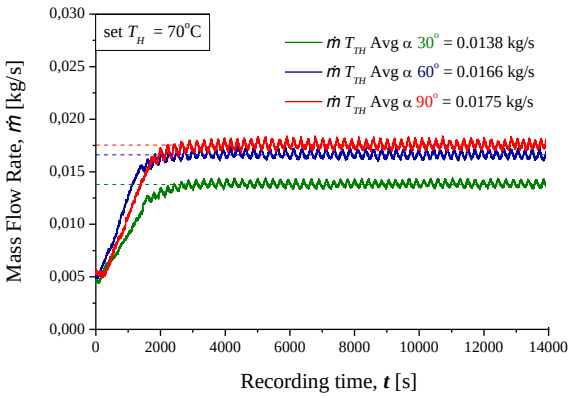

(b)

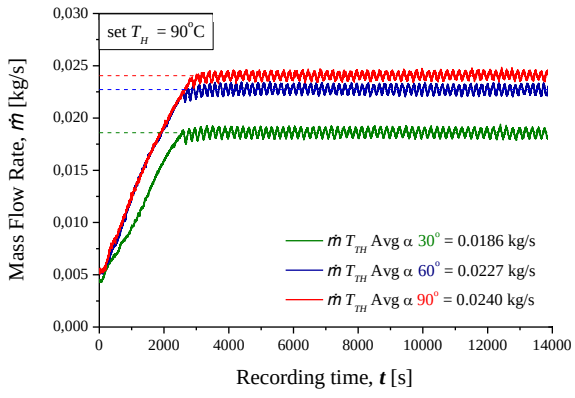

(c)

Fig. 13. Mass flow rate variation temperature characteristics inside pipe of WHT.

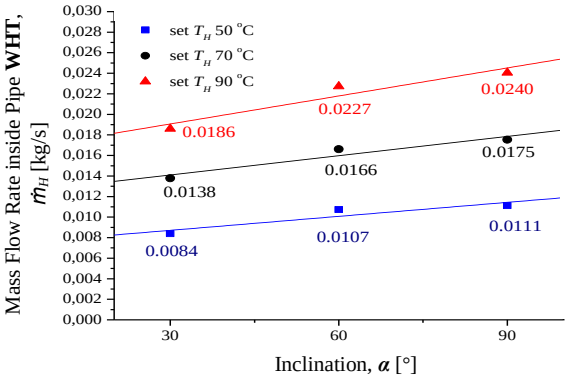

Fig. 14. Mass flow rate characteristics inside pipe of WHT.

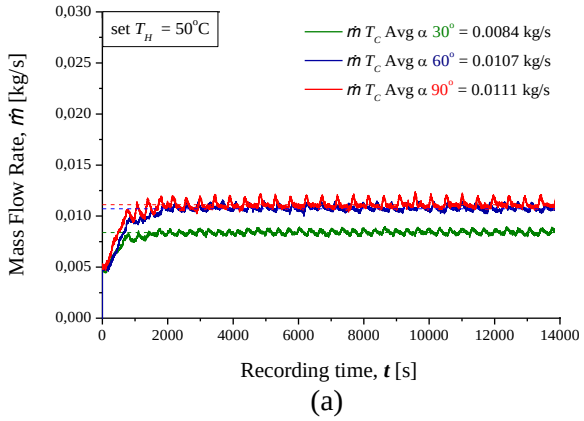

(a)

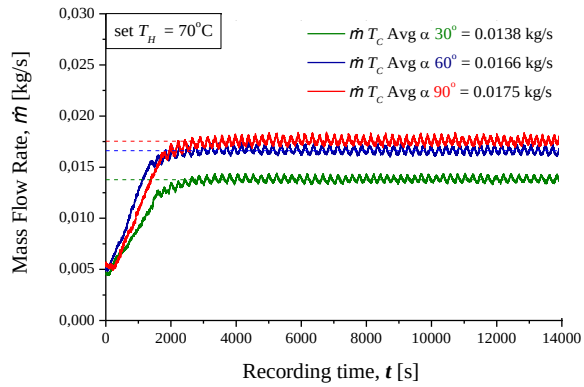

(b)

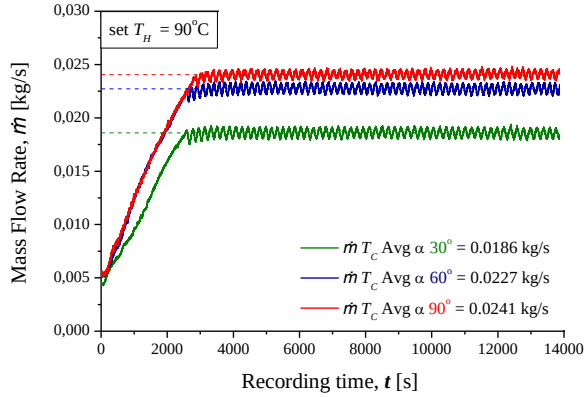

(c)

Fig. 15. Mass flow rate variation characteristics inside pipe of WCT.

Figure 14 shows that the mass flow rate was strongly influenced by both WHT temperature variations and loop inclination. The highest average mass flow rate occurred at the maximum WHT temperature and a 90° inclination, while the lowest was observed at 50°C and a 30° inclination. Changes in loop inclination increased the friction area along the fluid path, resulting in a reduction in mass flow rate. Additionally, increasing the WHT temperature led to a significant increase in the mass flow rate.

Experiments at different WHT input temperatures produced varying mass flow rates for each loop inclination angle. The results of the flow rate analysis in the WCT are shown in Fig. 15a.

At a WCT temperature of 50°C, the largest mass flow rate occurred at a loop inclination of 90°, with an average of 0.0111 kg/s, which also represented the highest mass flow rate at this WHT temperature. The mass flow rate at 30° differed from those at 60° and 90° by approximately ±0.0025 kg/s. The WCT mass flow rates followed the same pattern as observed in the WHT (Fig. 15b).

At a WHT temperature of 70°C, the largest mass flow rate in the WCT was 0.0175 kg/s at a loop inclination of 90°, while the smallest occurred at 30° (Fig. 15c).

Based on Fig. 15, the comparison of mass flow rates across all temperatures shows that the largest mass flow rate reached 0.0241 kg/s, while the smallest occurred at an inclination of 30°, with a difference of ±0.00485 kg/s between the 60° and 90° inclinations, as shown in Fig. 16.

The mass flow rate in the hot-leg is shown in Fig. 17a for a WHT temperature of 50°C. At a loop inclination of 90°, the largest average mass flow rate of 0.0111 kg/s was observed, while the smallest occurred at 30°. For a WHT temperature of 70°C (Fig. 17b), the largest mass flow rate of 0.0175 kg/s was recorded at 90°, and the smallest, 0.0138 kg/s, at 30°. At 90°C (Fig. 17c), the largest mass flow rate reached 0.0240 kg/s, while the smallest occurred at 30°, with a difference of ±0.00485 kg/s between the 60° and 90° inclinations.

Figure 18 shows the effect of WHT temperature variations and loop inclination on the mass flow rate in the hot-leg. The mass flow rate was strongly influenced by both variables, with an approximately proportional relationship between increasing WHT temperature and the hot-leg mass flow rate.

The cold-leg mass flow rate at a WHT temperature of 50°C (Fig. 19a) was highest at a loop inclination of 90°, with an average of 0.0111 kg/s, representing the largest mass flow rate at this temperature. The mass flow rate at 30° differed from those at 60° and 90° by approximately ±0.0025 kg/s. For a WHT temperature of 70°C (Fig. 19b), the largest mass flow rate of 0.0175 kg/s occurred at 90°, hile the

smallest, 0.0138 kg/s, was observed at 30°. At 90°C (Fig. 19c), the maximum mass flow rate reached 0.0241 kg/s, with the minimum at 30°, and a difference of ±0.00485 kg/s between the 60° and 90° inclinations.

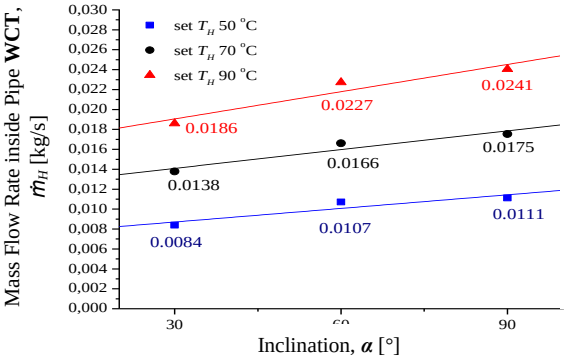

Fig. 16. Mass flow rate characteristics inside WCT.

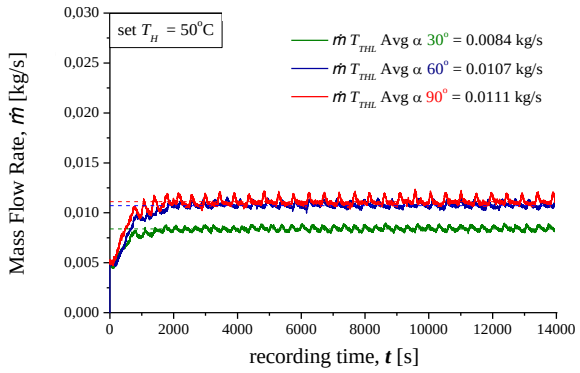

(a)

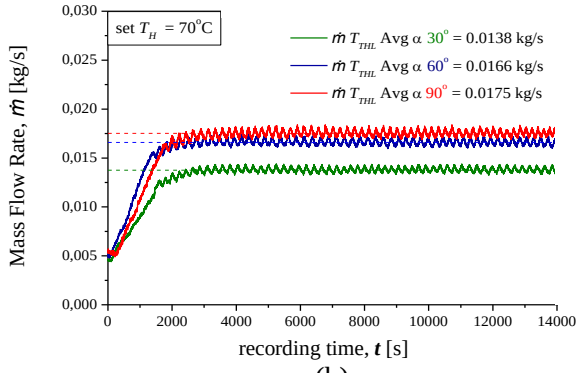

(b)

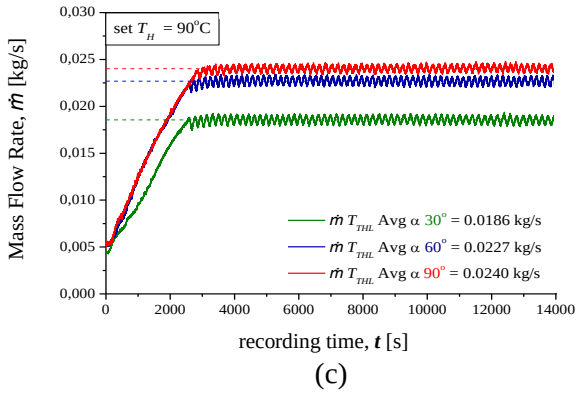

(c)

Fig. 17. Mass flow rate variation characteristics profile inside hot-leg.

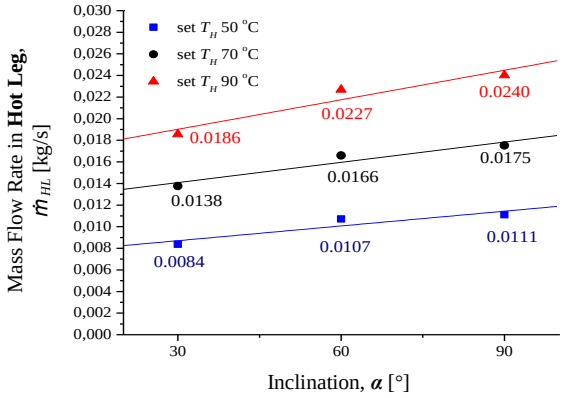

Fig. 18. Mass flow rate characteristics profile inside hot-leg.

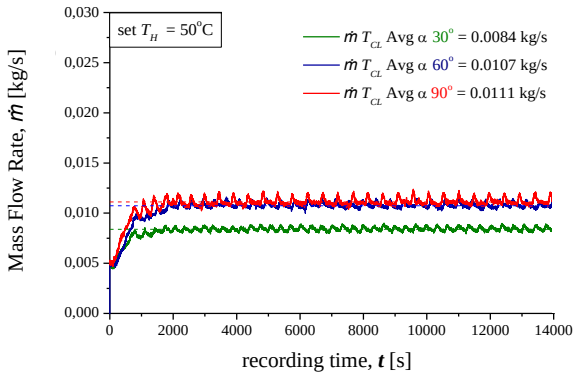

(a)

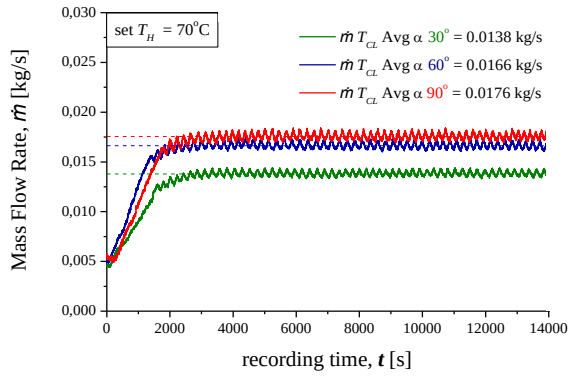

(b)

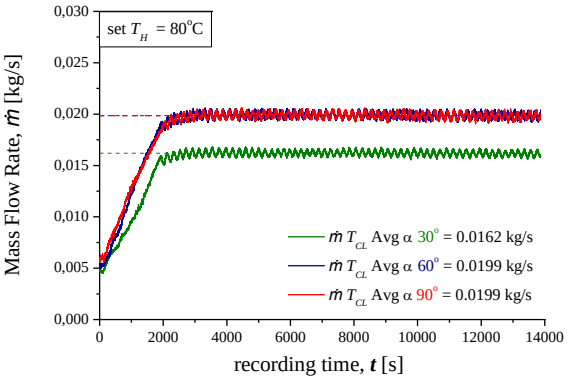

(c)

Fig. 19. Mass flow rate variation characteristics inside cold-leg.

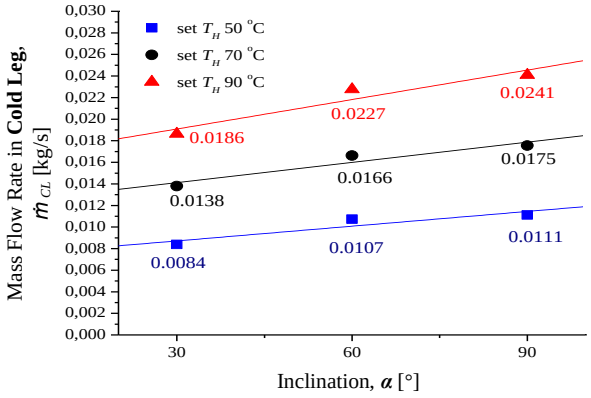

Fig. 20. Mass flow rate characteristics profile inside cold-leg.

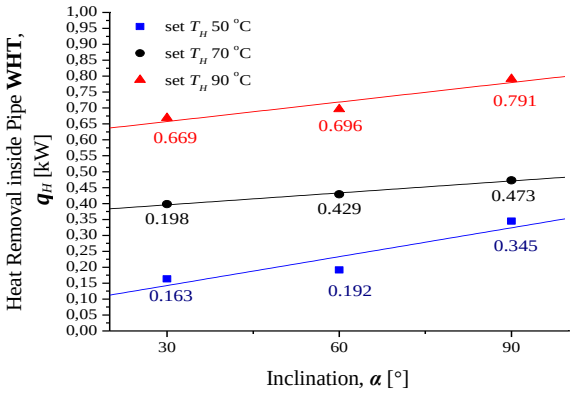

Fig. 21. Heat removal *qH*.

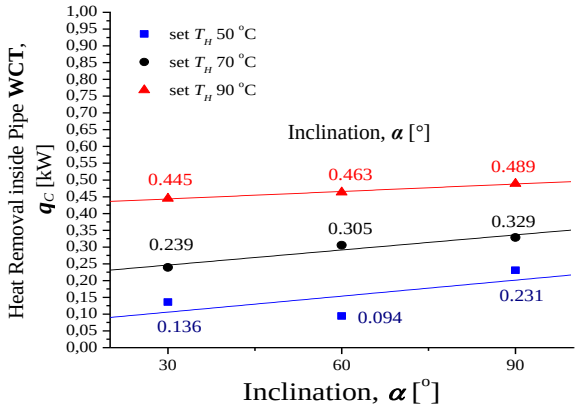

Fig. 22. Heat removal *qC*.

Figure 20 shows the effect of WHT temperature variations and loop inclination on the mass flow rate in the cold-leg. The mass flow rate was strongly influenced by both variables, with an approximately proportional relationship between increasing WHT temperature and the cold-leg mass flow rate. The mass flow rates calculated using Eqs. (2) and (3) were subsequently used to simplify the calculation of heat removal between the WHT and WCT in the loop for different slope angles.

Heat removal analysis

The discussion of heat removal is based on calculations using Eqs. (6) and (7), as well as supporting data obtained from Fig. 6 for the WHT and Fig. 8 for the WCT, for each variation in heating water temperature. The results, based on slope angle, are presented graphically in Fig. 21.

The heat removal in the WHT section was highest at a loop inclination of 90° for all temperature settings of 50°C, 70°C, and 90°C, as shown in Fig. 21. This is evident from the heat removal values for each inclination, which were influenced by the corresponding temperature differences ΔTH and by variations in dynamic viscosity, resulting in increased RFF forces with higher inclinations. The maximum heat removal occurred at a WHT temperature of 90°C and an inclination of 90°.

The heat removal in the WCT section was highest at a loop inclination of 90° for all temperature settings of 50°C, 70°C, and 90°C. In contrast, the lowest heat removal occurred at an inclination of 30°. An exception was observed at the 50°C setting, where the inclination of 60° resulted in a comparatively low heat transfer value, as shown in Fig. 22.

CONCLUSION

The characteristics of temperature differences show that heat removal occurs by free convection and natural circulation. In the case of a temperature of 50°C, the heat removal is mostly free convection; the fluid does not move, and the mass of the fluid does not move predominantly still in a state of free convection so that the heat removal from the WHT temperature to the WCT with a slope of 30° causes a large heat loss effect. Then, at a temperature setting of 70°C and 90°C, each inclination means that heat removal occurs by free convection and natural circulation. The mass flow rate increases with each increase in the heater temperature setting.

The research results show that the increase in natural circulation mass flow rate and heat removal capability is influenced by increasing the loop inclination and water temperature in the heating tank. It was found that the loop condition with an inclination of 90° and a temperature setting of 90°C had a higher value, namely in each section. is $\dot{m}$ = 0.0241 kg/s for mass flow rate and qH = 0.791 kW, qC= 0.489 kW, for heat removal. The resulting buoyancy force becomes stronger, resulting in heat removal through natural circulation flow, greater than free convection, thereby increasing the mass flow rate and heat removal.

NOMENCLATURE

A	: area of inner pipe (m^2)
c_p	: specific heat of liquid at constant pressure (J/kg.K)
I	: current (Ampere)
$\dot{m}$	: mass flowrate (kg/s)
$\dot{m}_c$	: mass flowrate inside pipe WCT (kg/s)
m_{CL}	: mass flowrate in cold leg (kg/s)
$\dot{m}_H$	: mass flowrate inside pipe WHT (kg/s)
$\dot{m}_{HL}$	: mass flowrate in hot leg (kg/s)
P	: power heater (Watt)
Q	: natural circulation flowrate (L/m)
q_C	: heat removal inside pipe WCT (Watt)
q_{CL}	: heat removal in cold leg (Watt)
q_H	: heat removal inside pipe WHT (Watt)
q_{HL}	: heat removal in hot leg (Watt)
T	: temperature (^oC)
T_C	: temperature inside pipe WCT (^oC)
T_{CL}	: temperature in cold leg (^oC)
T_F	: temperature fluida (^oC)
T_H	: temperature inside pipe WHT (^oC)
T_{HL}	: Temperature in hot leg (^oC)
v	: velocity (m/s)
V	: voltage (volt)
ΔT_C	: temperature difference inlet outlet WCT (^oC)
ΔT_{CL}	: temperature difference outlet WHT inlet WCT(^oC)
ΔT_H	: temperature difference inlet outlet WHT (^oC)
ΔT_{HL}	: temperature difference outlet WCT inlet WHT(^oC)
α	: inclination (^{o})
ρ	: density of water (kg/m^3)
ρ_{Th}	: density of water in heater (kg/m^3)
FASSIP	: *Fasilitas Simulasi SIstem Pasif*
HHHC	: horizontal heater horizontal cooler
HHVC	: horizontal heater vertical cooler
LWRs	: light water reactors
NCL	: natural circulation loop
NI	: national instrument
NPP	: nuclear power plant
PCS	: passive cooling system
SBO	: station blackout
SR	: richter scale
VHHC	: vertical heater horizontal cooler
VHVC	: vertical heater vertical cooler
WCT	: water cooling tank
WHT	: water heating tank

ACKNOWLEDGMENT

The authors wish to thank you because the Program of Riset Inovasi untuk Indonesia Maju (RIIM) batch-1 LPDP Mandatori BRIN funded this research with contract numbers B-811/II.7.5/FR/6/2022 and B-2103/III. 2/HK. 04.03/7/2022. Thank you to the Head of the Research Center for Nuclear Reactor Technology, the Research Organization for Nuclear Energi (BATAN), and the National Research and Innovation Agency (BRIN) for supporting these research activities. Also, thanks to the Nuclear Reactor Thermal-Fluids System (NRTFSys.) research group colleagues for supporting these research activities.

AUTHOR CONTRIBUTION

Nur Rochman Budiyanto: Research method, experiment, calculation and analysis data, manuscript wrating. Mulya Juarsa and Deendarlianto: Ide/Concepts, Manuscript review, funding, and as a research guidance for first author during the magister program. Other authors: Experimental and data collecting.

REFERENCES

1. Y. Kim, M. Kim, and W. Kim, Energy Policy **61** (2013) 822.
2. S. Yoshimura, T. Yamaguchi, K. Ino *et al*., Nucl. Eng. Des. **380** (2021) 111293.
3. M. Juarsa, A. R. Antariksawan, M. H. Kusuma et al., *Estimation of natural circulation flow based on temperature in the FASSIP-02 large-scale test loop facility*, in: IOP Conf. Ser. Earth Environ. Sci. **105** (2018) 012091.
4. P. K. Vijayan and A. W. Date, Nucl. Eng. Des. **136** (1992) 361.
5. R. B. Duffey and J. P. Sursock, Nucl. Eng. Des. **102** (1987) 115.
6. M. Juarsa, J. P. Witoko, Giarno *et al.,* Atom Indones. **44** (2018) 123.
7. H. Cheng, H. Lei, L. Zeng *et al.,* Int. J. Heat Mass Transf. **128** (2019) 208.
8. M. Juarsa, J. H. Purba, H. M. Kusuma *et al.*, Atom Indones. **40** (2014) 141.
9. D. N. Elton, U. C. Arunachala, and P. K. Vijayan, Int. Commun. Heat Mass Transf. **137** (2022) 106216.
10. M. Juarsa, Giarno, A. N. Rohman *et al.*, *Flow Rate and Temperature Characteristics in Steady State Condition on FASSIP-01 Loop During Commissioning*, IOP Conf. Series: Journal of Physics: Conf. Series **962** (2018) 012021.
11. P. K. Vijayan, Nucl. Eng. Des. **215** (2002) 139.
12. P. K. Vijayan, M. Sharma, and D. Saha, Exp. Therm. Fluid Sci. **31** (2007) 925.
13. International Atomic Energy Agency (IAEA), Passive Safety Systems in Advanced Water Cooled Reactors (AWCRs), IAEA, Vienna (2013).
14. E. P. Ariesta, Deendarlianto, A. S. Al Amin *et al.,* Atom Indones. **50** (2024) 201.
15. C. Cheng, D. Lu, Q. Su *et al*., Nucl. Eng. Des. **402** (2023) 112122.
16. L. Chen, X.R. Zhang, and B. Jiang, J. Heat Transfer **136** (2014) 1.

17. M. Sharma, D. S. Pilkhwal, P. K. Vijayan *et al.*, Heat Transfer Eng. **33** (2012) 809.
18. B. T. Swapnalee, P. K. Vijayan, M. Sharma *et al.*, Nucl. Eng. Des. **245** (2012) 99.
19. L. Chen, B. L. Deng, X. R. Zhang, Appl. Therm. Eng. **59** (2013) 1.
20. M. Misale, P. Garibaldi, J. C. Passos *et al.*, Exp. Therm. Fluid Sci. **31** (2007) 1111.
21. M. Krishnani and D. N. Basu, Ann. Nucl. Energy **107** (2017) 17.
22. T. Srivastava, D. N. Basu, Nucl. Eng. Des. **390** (2022) 111704.
23. Y. S. Gaos, M. Juarsa, E. Marzuki *et al* ., Jurnal Teknologi Reaktor Nuklir Tri Dasa Mega, **14** (2012) 39. (in Indonesian)
24. M. Misale, F. Devia, and P. Garibaldi, Appl. Therm. Eng. **40** (2012) 64.
25. M. Sahu, J. Sarkar, and L. Chandra, Int. J. Therm. Sci. **187** (2023) 108198.
26. A. Crabtree and M. Siman-Tov, Thermophysical Properties of Saturated Light and Heavy Water for Advanced Neutron Source Applications, Oak Ridge National Laboratory (ORNL), Oak Ridge (1993).